



# Ultrasonic-assisted deposition of Ni-P-Al<sub>2</sub>O<sub>3</sub> coating for practical protection of mild steel: Influence of ultrasound frequency on the corrosion behavior of the coating

Habib Ashassi-Sorkhabi\*, Jafar Mostafaei, Amir Kazempour, Elnaz Asghari

*Electrochemistry Research Laboratory, Department of Physical Chemistry, Faculty of Chemistry, University of Tabriz, Tabriz, Iran*

## ARTICLE INFO

### Article history:

Received 10 April 2022  
 Received in revised form 5 May 2022  
 Accepted 8 May 2022  
 Available online 8 May 2022

### Keywords:

Ni-P nanocomposite coating  
 Sonoelectroless  
 Corrosion  
 Ultrasound wave frequency

## ABSTRACT

In this paper, the precipitation of nickel-phosphorous (Ni-P) electroless coatings including Al<sub>2</sub>O<sub>3</sub> nanoparticles (Ni-P-NA) using ultrasound waves on mild steel has been studied. Deposition process occurred in a lactic plating bath by the autocatalytic method using an ultrasound probe. The effect of radiation frequency on the properties of coatings was investigated, and the optimum frequency was determined. The obtained samples were evaluated for their corrosion resistance, surface morphology, and hardness by electrochemical impedance spectroscopy (EIS), potentiodynamic polarization, and scanning electron microscopy (SEM). The results showed that ultrasound waves caused an improvement in the corrosion resistance and uniformity of the coatings. Furthermore, five different wave frequencies applied during deposition disclosed the remarkable impact of frequency on the smoothness and corrosion resistance of the resultant coatings. On this basis, the Nyquist diagrams showed that the corrosion resistance of the prepared Ni-P-NA coating at an optimum frequency of 75 kHz was 2.59 kΩ·cm<sup>2</sup>. This value was about 2.5 times higher than the value obtained for the Ni-P-NA coating deposited without ultrasound power.

## 1. Introduction

Electroless nickel precipitation is broadly used in various industries, such as electronics, automotive, aerospace, medicine, petrochemical, food, and military industries. These wide applications can be explained by a precise understanding of several properties, including corrosion resistance, high abrasion resistance, uniform coating thickness, and magnetic properties [1]. The electroless method is an excellent way to cover complex parts [2]. The electroless nickel coating process has led to the widespread growth of surface engineering [3], and because of its unique physical and chemical properties, it has usually replaced hard chrome coatings [4]. Its corrosion resistance is excellent, and in most environments, it is better than pure nickel or chromium [5,6]. In addition, the electroless nickel coating has a high coating ability, high strength bonds, good anti-abrasion properties, corrosion resistance, excellent welding capability, good thermal and electrical conductivity, and magnetic properties that can be

controlled by heat treatment [7]. In addition to pure Ni coatings, composite coatings are created by adding fine particles in powder form to the plating solution and suspension (deposition) of these particles and their simultaneous deposition along with electroless nickel-based coatings. In this way, due to the juxtaposition of two or more phases, a set of properties is obtained that cannot be achieved by individual components [8]. In addition to hardness and abrasion resistance, good corrosion resistance of the coating is one of the other properties affected by the presence of these particles in the coating [9].

The ultrasound in electrochemistry has been used in various fields, such as sonoanalysis, sonoelectrosynthesis, sonoelectrodeposition, accelerating corrosion studies, wastewater treatment, etc. Ultrasonic radiation brings energy into the system and increases mass transfer due to acoustic microcurrents and cavitation phenomena, especially in the strong ultrasound region (20-100 kHz) [10]. The study of the effect of ultrasound on electrocoating has been one of the first

\*Corresponding author. Email: [habib.ashassi@gmail.com](mailto:habib.ashassi@gmail.com)

active topics in sonoelectrochemistry. The benefits of ultrasound are well established and have been used consistently [11]. Not only metal coatings such as Ag [12] and W [13], but bioactive calcium phosphate ( $\text{CaPO}_4$ ) coatings [14], CdSe films [15], and  $\text{Ag}_2\text{O}$  [16] are also sonoelectro-assembled. In addition, other surface applications have been improved by the use of sonoelectrochemistry, such as anodizing [17], etching [18], sonoelectropolymerization [19], sonoelectrodeposition [20], and composite electrodes [21]. The use of ultrasound during the plating of composite coatings significantly improves the hardening effect [22]. The results reported by Indyka et al [23,24] showed that not only the presence of ultrasound during the plating process significantly reduced the accumulation of particles and led to a more uniform dispersion in the composite, but also the frequency of ultrasound radiation was an effective parameter. The study of the power of ultrasound applied in the sonoelectrodeposition process has been done by different research groups. The results of their studies show that the use of high ultrasonic powers increases the amount of nanoparticles in the final coatings. However, they also showed that there is a maximum value in the amount of ultrasound power applied so that a further increase in power reduces the amount of particles in the coating [25].

In this paper, an ultrasound wave (with different frequencies) was employed to agitate Ni-P electroless solutions to produce Ni-P and Ni-P- $\text{Al}_2\text{O}_3$  coatings on mild steel. The microstructures, hardness, and corrosion resistance of the deposits were compared with those that plated without ultrasound.

## 2. Results and Discussion

### 2.1. XRD patterns of the prepared coatings

The XRD patterns of the Ni-P coating with and without alumina nanoparticles deposited under ultrasonic waves with a frequency of 75 kHz are shown in Fig. 1. A wide peak appeared at  $45^\circ$  for both of the coatings is the characteristic peak of Ni-P coatings, showing a typical semi-crystalline phase, which demonstrates a mixture of crystallized and amorphous structures. It can be found from the XRD pattern that the incorporation of alumina does not affect the coating structure even though it may change the morphology of the Ni-P coating.

### 2.2. SEM and EDS analyses of the coatings

Fig. 2 depicts the effect of alumina nanoparticles on the surface morphology of the Ni-P coating synthesized under ultrasonic agitation with a frequency of 75 kHz. The Ni-P-NA coating has a rough surface and provides a nodular structure all over the surface.

It has been reported that the presence of nanoparticles increases the coating hardness, resulting in improved corrosion resistance of the coating. On this

basis, the micro hardness of the Ni-P coating increased from 578.0 to 613.7  $\text{HV}_{50}$  after the incorporation of alumina nanoparticles. The EDS analysis of the coatings is also given in Fig. 2. From this figure, the Al peak can be observed in the EDS, which demonstrates the presence of alumina nanoparticles in the Ni-P coating.

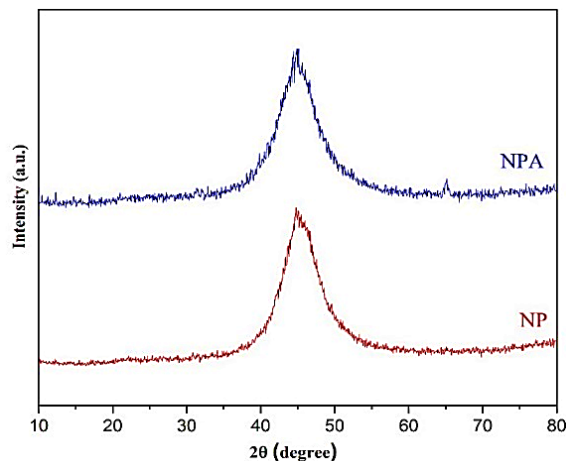


**Fig. 1.** XRD patterns of the electroless Ni-P (determined as NP) and Ni-P-NA (determined as NPA) coatings deposited under ultrasound wave with the frequency of 75 kHz.

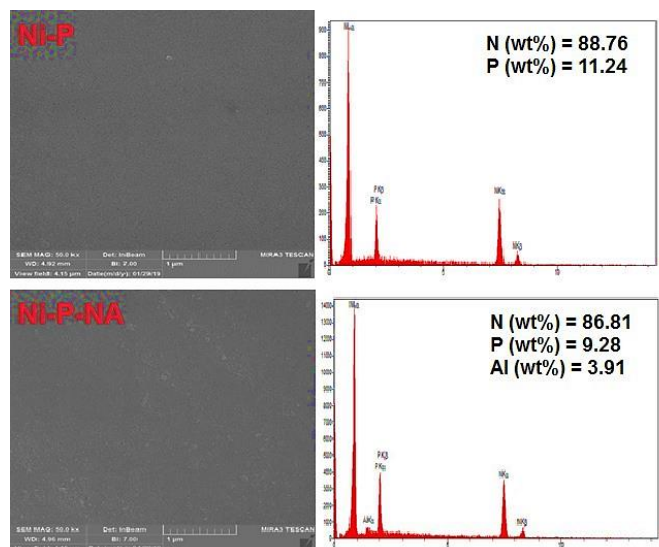


**Fig. 2.** SEM and EDX analyses of the electroless Ni-P and Ni-P-NA coatings deposited under ultrasound with the frequency of 75 kHz.

### 2.3. EIS results

The Nyquist diagrams of the Ni-P and Ni-P-NA coatings deposited under ultrasonic power with frequencies of 0, 25, 50, 75, 100, and 150 kHz are depicted in Fig. 3. In these diagrams, two time constants were detected in which the first time constant is attributed to the Ni-P coating, as evidenced by a loop appearing at high frequencies. This time constant includes  $R_{\text{coat}}$  and

$CPE_{\text{coat}}$ , which describe the coating resistance and constant phase element, respectively. The second time constant that appeared as a loop at intermediate frequencies corresponds to the double-layer. This time constant is explained by  $CPE_{\text{dl}}$ , which represents the double-layer constant phase element, and  $R_{\text{ct}}$ , which shows the charge transfer resistance of the steel.  $R_s$  is also introduced as the solution resistance. The obtained experimental Nyquist plots were fitted by the equivalent circuit shown in Fig. 4, and the resulting parameters were collected in Table 1.

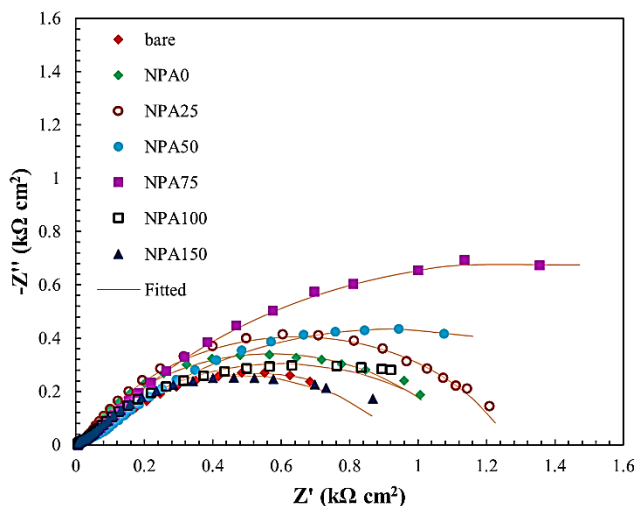
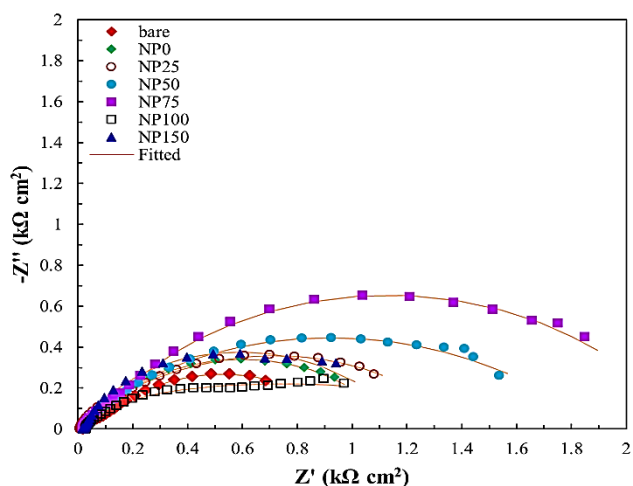


**Fig. 3.** Nyquist plots of the electroless Ni-P (determined as NP) and Ni-P-NA (determined as NPA) coatings fabricated under ultrasound with various frequencies.

The data included in this table revealed that the deposition of Ni-P coating under any condition has remarkably improved the corrosion resistance of the bare steel. Furthermore, the incorporation of alumina nanoparticles into the coating improved the resistance of the Ni-P coating. This could be due to an increase in the microhardness and a decrease in the porosity of the

deposited coating after the addition of  $\text{Al}_2\text{O}_3$  nanoparticles to the bath. According to Table 1, the corrosion resistance of the coatings deposited under ultrasonic agitation is higher than that of the coatings prepared without ultrasound. Additionally, the variation of ultrasound frequency affected the surface properties of the synthesized coatings. On this basis, the corrosion resistance of the coatings improved with increasing the ultrasound frequency from 25 to 75 kHz but then reduced with further increase of frequency. For example, the polarization resistance ( $R_p = R_{\text{coat}} + R_{\text{ct}}$ ) of the Ni-P-NA coating increased from  $1128 \Omega \cdot \text{cm}^2$  at the condition without ultrasound to  $2588 \Omega \cdot \text{cm}^2$  under ultrasonic agitation with the optimum frequency (75 kHz).

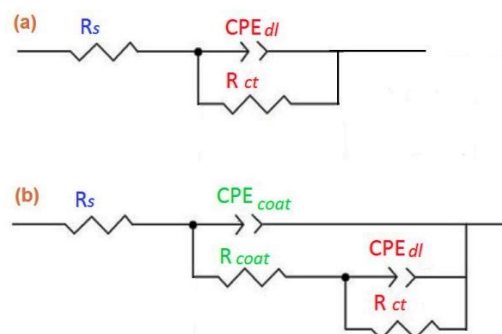


**Fig. 4.** Equivalent circuit models used to fit the experimental Nyquist diagrams. Circuit (a) was employed for bare steel and circuit (b) was applied for coated samples.

#### 2.4. Potentiodynamic polarization results

The polarization plots of the Ni-P and Ni-P-NA coatings prepared under ultrasonic agitation with the optimum frequency of 75 kHz were provided and represented in Fig. 5. The obtained Tafel plots were analyzed to obtain corrosion potential ( $E_{\text{corr}}$ ), corrosion current density ( $i_{\text{corr}}$ ), and Tafel slopes ( $b_a$  and  $b_c$ ), which are given in Table 2. According to this table, all the coated samples exhibit better performance than the bare steel. This means a reduction in the corrosion current densities of the coated samples. Such a result indicates that the deposited coatings have successfully protected the underlying substrate from corrosion. Table 2 shows that the coatings synthesized under 75 kHz ultrasound exhibit lower corrosion current densities. This observation is in line with the values of polarization resistance ( $R_p$ ), where the  $R_p$  values of Ni-P and Ni-coatings prepared at the frequency of 75 kHz were higher than those of the same coatings synthesized without ultrasound.

**Table 1.** Electrochemical impedance parameters obtained for electroless Ni-P and Ni-P-NA coatings prepared under ultrasound with various frequencies.

Sample	Ultrasound frequency (kHz)	CPE <sub>coat</sub>		R <sub>coat</sub> (Ω cm <sup>2</sup> )	CPE <sub>dl</sub>		R <sub>ct</sub> (Ω cm <sup>2</sup> )	R <sub>total</sub> (Ω cm <sup>2</sup> )	Fitting error
		Y <sub>0</sub> ×10 <sup>-5</sup> (Ω <sup>-1</sup> cm <sup>-2</sup> S <sup>n</sup> )	n		Y <sub>0</sub> ×10 <sup>-4</sup> (Ω <sup>-1</sup> cm <sup>-2</sup> S <sup>n</sup> )	n			
bare	-	-	-	-	9.28	0.66	887	887.00	0.00006
Ni-P	0	8.41	0.90	90.09	4.96	0.67	1063	1153.09	0.00038
	25	7.50	0.90	111.9	4.18	0.68	1198	1309.90	0.00012
	50	6.03	0.90	120.2	4.05	0.72	1774	1894.20	0.00036
	75	5.24	0.92	167.8	3.00	0.76	2042	2209.80	0.00034
	100	8.27	0.85	56.27	6.53	0.62	1760	1816.27	0.00037
	150	9.06	0.64	20.62	5.22	0.67	1175	1195.62	0.00013
	Ni-P-NA	0	75.03	0.64	39.43	2.90	0.84	1089	1128.43
25		11.43	0.76	33.73	3.70	0.72	1228	1261.73	0.00042
50		10.01	0.79	53.10	17.88	0.58	1738	1791.10	0.00040
75		9.70	0.86	39.27	14.13	0.61	2549	2588.27	0.00034
100		5.35	0.89	22.03	14.92	0.60	1157	1179.03	0.00067
150		7.51	0.88	35.95	10.36	0.64	912	947.55	0.00087

**Table 2.** Potentiodynamic polarization parameters obtained for electroless Ni-P and Ni-P-NA coatings produced without ultrasound and under ultrasonic agitation with the frequency of 75 kHz.

Sample	Ultrasound frequency (kHz)	E <sub>corr</sub> (mV vs. Ag/AgCl)	i <sub>corr</sub> (μA/cm <sup>2</sup> )	b <sub>a</sub> (mV/dec)	b <sub>c</sub> (mV/dec)	R <sub>p</sub> (kΩ cm <sup>2</sup> )
bare	-	-480.38	13.63	82.19	178.53	1.79
Ni-P	0	-472.70	10.12	95.10	117.76	2.25
	75	-414.45	6.44	94.62	94.59	3.18
Ni-P-NA	0	-541.63	9.52	73.96	170.17	2.35
	75	-546.68	3.42	68.65	114.39	5.43

### 3. Experimental

#### 3.1. Chemicals

The materials used here were nickel sulfate (NiSO<sub>4</sub>·6H<sub>2</sub>O), sodium acetate (CH<sub>3</sub>COONa), sodium hypophosphite (NaH<sub>2</sub>PO<sub>2</sub>), lactic acid (NaC<sub>6</sub>H<sub>3</sub>O<sub>7</sub>), thiourea (CH<sub>4</sub>N<sub>2</sub>S), tween 20 as a surfactant (C<sub>58</sub>H<sub>114</sub>O<sub>26</sub>), alumina nano powder, and sodium chloride (NaCl). All the materials were purchased from Merck and used as received.

#### 3.2. Instruments

The chemical compositions of the coatings were determined using an energy-dispersive X-ray spectroscopy (EDX) system attached to the SEM. The X-ray diffraction (XRD) patterns of the coated samples were prepared by a Siemens D5000 X-ray diffractometer. The microhardness of the coatings was measured using an HV-1000Z microhardness tester. The ultrasonic probe used for the synthesis was Dr. Hielscher GmbH, up to 400 s. The electrochemical tests were carried out using a PGSTAT30 Autolab.

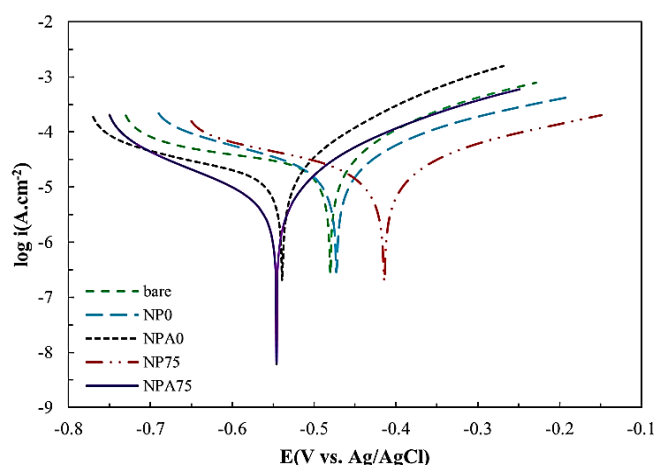


**Fig. 5.** Tafel plots provided for the electroless Ni-P and Ni-P-NA coatings synthesized under ultrasound with the frequency of 75 kHz (NP75 and NPA75) and without ultrasound (NP0 and NPA0).

### 3.3. Deposition of Ni-P coatings with and without $Al_2O_3$ nanoparticles

First of all, the mild steel sheets with a surface area of  $1 \times 1 \text{ cm}^2$  were abraded by SiC papers and then initially cleaned using distilled water. To remove any dirt or grease substance from the steel surface, the sheets were immersed in hot NaOH solution (1 M) for about 3 min and then washed with acetone and distilled water. Furthermore, the acid treatment of 30% HCl was proceeded for 1 min to remove oxide layers from the surface. Eventually, the samples were rinsed with distilled water and immersed in the deposition bath containing  $30 \text{ g}\cdot\text{L}^{-1} \text{ NiSO}_4\cdot 6\text{H}_2\text{O}$ ,  $30 \text{ g}\cdot\text{L}^{-1} \text{ NaH}_2\text{PO}_2$ ,  $45 \text{ g}\cdot\text{L}^{-1} \text{ CH}_3\text{COONa}$ ,  $25 \text{ mL}\cdot\text{L}^{-1} \text{ NaC}_6\text{H}_3\text{O}_7$ ,  $0.005 \text{ g}\cdot\text{L}^{-1} \text{ CH}_4\text{N}_2\text{S}$ , and  $0.003 \text{ g}\cdot\text{L}^{-1}$  tween 20. To prepare Ni-P-NA coatings, 20 ppm  $Al_2O_3$  nanoparticles were added to the deposition bath. Ultrasonic waves from 0 to 150 kHz were imposed to the bath during 1 h electroless deposition. The bath temperature was kept constant at  $90 \text{ }^\circ\text{C}$ , and the pH of the bath was adjusted to 4.8 using dilute solutions of  $\text{H}_2\text{SO}_4$  and NaOH.

### 3.4. Electrochemical tests

The corrosion behavior of the synthesized coatings was evaluated in 3.5% NaCl solution by electrochemical impedance spectroscopy (EIS) and potentiodynamic polarization (PDP). All the measurements were done in a three-electrode cell containing a mounted mild steel coupon, a platinum wire,

and an Ag/AgCl (saturated KCl) electrode as the working, counter, and reference electrodes, respectively. The frequency in EIS measurement ranged from 10 kHz to 10 mHz with a voltage perturbation amplitude of 10 mV. PDP plots were provided in a potential range of -250 to 250 mV versus open circuit potential at a scan rate of  $1 \text{ mV}\cdot\text{s}^{-1}$ .

## 4. Conclusion

This work evaluated the influence of ultrasound frequency on the corrosion resistance of Ni-P coating in the absence and presence of alumina nanoparticles. The results obtained indicated that the corrosion resistance of the Ni-P coatings improved when deposition was performed under ultrasound power. Moreover, the properties of the coatings synthesized under different ultrasound frequencies varied in such a way that the best performance was observed for the coatings deposited under the frequency of 75 kHz.

## Acknowledgements

The authors would like to thank the University of Tabriz for the financial support of the present work.

## References

- [1] L. Bonin, N. Bains, V. Vitry, A.J. Cobley, Electroless deposition of nickel-boron coatings using low frequency ultrasonic agitation: Effect of ultrasonic frequency on the coatings, *Ultrasonics*. 77 (2017) 61–68.
- [2] M.S. Hussain, T.E. Such, Deposition of composite autocatalytic nickel coatings containing particles, *Surf. Technol.* 13 (1981) 119–125.
- [3] R.C. Agarwala, V. Agarwala, Electroless alloy/composite coatings: A review, *Sadhana*. 28 (2003) 475–493.
- [4] J.R. Davis, *Surface engineering for corrosion and wear resistance*, ASM international, 2001.
- [5] I. Apachitei, F.D. Tichelaar, J. Duszczyk, L. Katgerman, The effect of heat treatment on the structure and abrasive wear resistance of autocatalytic NiP and NiP-SiC coatings, *Surf. Coatings Technol.* 149 (2002) 263–278.
- [6] H. Ashassi-Sorkhabi, S.H. Rafizadeh, Effect of coating time and heat treatment on structures and corrosion characteristics of electroless Ni-P alloy deposits, *Surf. Coatings Technol.* 176 (2004) 318–326.
- [7] L.-G. Yu, X.-S. Zhang, The friction and wear properties of electroless Ni-polytetrafluoroethylene composite coating, *Thin Solid Films*. 245 (1994) 98–103.
- [8] E. Pena-Munoz, P. Bercot, A. Grosjean, M. Rezrazi, J. Pagetti, Electrolytic and electroless coatings of Ni-PTFE composites: Study of some characteristics, *Surf.*

- Coatings Technol. 107 (1998) 85–93.
- [9] A.S. Hamdy, M.A. Shoeib, H. Hady, O.F.A. Salam, Corrosion behavior of electroless Ni–P alloy coatings containing tungsten or nano-scattered alumina composite in 3.5% NaCl solution, *Surf. Coatings Technol.* 202 (2007) 162–171.
- [10] V. Sáez, T.J. Mason, Sonoelectrochemical synthesis of nanoparticles, *Molecules.* 14 (2009) 4284–4299.
- [11] A. Brotchie, F. Grieser, M. Ashokkumar, The role of salts in acoustic cavitation and the use of inorganic complexes as cavitation probes, in: *Theor. Exp. Sonochemistry Invol. Inorg. Syst.*, Springer, 2010: pp. 357–379.
- [12] B. Pollet, J.P. Lorimer, S.S. Phull, J.Y. Hihn, Sonoelectrochemical recovery of silver from photographic processing solutions, *Ultrason. Sonochem.* 7 (2000) 69–76.
- [13] C.H. Goeting, J.S. Foord, F. Marken, R.G. Compton, Sonoelectrochemistry at tungsten-supported boron-doped CVD diamond electrodes, *Diam. Relat. Mater.* 8 (1999) 824–829.
- [14] H.M. Han, G.J. Phillips, S. V Mikhailovsky, S. FitzGerald, A.W. Lloyd, Sonoelectrochemical deposition of calcium phosphates on carbon materials: effect of current density, *J. Mater. Sci. Mater. Med.* 19 (2008) 1787–1791.
- [15] K.R. Murali, P. Sasindran, Structural and optical properties of sonoelectrochemically deposited CdSe films, *J. Mater. Sci.* 39 (2004) 6347–6348.
- [16] A.J. Saterlay, S.J. Wilkins, C.H. Goeting, J.S. Foord, R.G. Compton, F. Marken, Sonoelectrochemistry at highly boron-doped diamond electrodes: silver oxide deposition and electrocatalysis in the presence of ultrasound, *J. Solid State Electrochem.* 4 (2000) 383–389.
- [17] S.K. Mohapatra, K.S. Raja, M. Misra, V.K. Mahajan, M. Ahmadian, Synthesis of self-organized mixed oxide nanotubes by sonoelectrochemical anodization of Ti–8Mn alloy, *Electrochim. Acta.* 53 (2007) 590–597.
- [18] J. Kang, Y. Shin, Y. Tak, Growth of etch pits formed during sonoelectrochemical etching of aluminum, *Electrochim. Acta.* 51 (2005) 1012–1016.
- [19] D. Reyman, E. Guereca, P. Herrasti, Electrodeposition of polythiophene assisted by sonochemistry and incorporation of fluorophores in the polymeric matrix, *Ultrason. Sonochem.* 14 (2007) 653–660.
- [20] C.-W. Lee, R.G. Compton, J.C. Eklund, D.N. Waller, Mercury-electroplated platinum electrodes and microelectrodes for sonoelectrochemistry, *Ultrason. Sonochem.* 2 (1995) S59–S62.
- [21] M.A. Murphy, F. Marken, J. Mocak, Sonoelectrochemistry of molecular and colloidal redox systems at carbon nanofiber–ceramic composite electrodes, *Electrochim. Acta.* 48 (2003) 3411–3417.
- [22] I. Tudela, Y. Zhang, M. Pal, I. Kerr, A.J. Cobley, Ultrasound-assisted electrodeposition of composite coatings with particles, *Surf. Coatings Technol.* 259 (2014) 363–373.
- [23] E. Beltowska-Lehman, P. Indyka, A. Bigos, M. Kot, L. Tarkowski, Electrodeposition of nanocrystalline Ni–W coatings strengthened by ultrafine alumina particles, *Surf. Coatings Technol.* 211 (2012) 62–66.
- [24] P. Indyka, E. Beltowska-Lehman, M. Bieda, J. Morgiel, L. Tarkowski, Microstructure and deposition relations in alumina particle strengthened Ni–W matrix composites, in: *Solid State Phenom.*, Trans Tech Publ, 2012: pp. 234–238.
- [25] H.-Y. Zheng, M.-Z. An, Electrodeposition of Zn–Ni–Al<sub>2</sub>O<sub>3</sub> nanocomposite coatings under ultrasound conditions, *J. Alloys Compd.* 459 (2008) 548–552.